DTU Library

Immittance-based Black-Box Model Identification via Vector Fitting Methods for Offshore Wind Power Plant Components

Haugaard, Jeppe; Malmquist, Finnur; Ghimire, Sulav; Gomes Guerreiro, Gabriel Miguel; Guest, Emerson; Yang, Guangya

Publication date:
2024

Document Version
Publisher's PDF, also known as Version of record

Citation (APA):
Haugaard, J., Malmquist, F., Ghimire, S., Gomes Guerreiro, G. M., Guest, E., & Yang, G. (2024). *Immittance-based Black-Box Model Identification via Vector Fitting Methods for Offshore Wind Power Plant Components*. Paper presented at 23rd Wind & Solar Integration Workshop, Helsinki, Finland.

Immittance-based Black-Box Model Identification via Vector Fitting Methods for Offshore Wind Power Plant Components

Jeppe Haugaard[1,2], Finnur Malmquist[1,2], Sulav Ghimire[1,2] , Gabriel M.G. Guerreiro[1,2], Emerson Guest[1], Guangya Yang[2]*

[1]*Siemens Gamesa Renewable Energy A/S, 7330 Brande, Denmark*
[2]*Department of Wind and Energy Systems, Technical University of Denmark, 2800 Kgs Lyngby, Denmark*
**E-mail: sulav.ghimire@siemensgamesa.com*

Keywords: Black-box models, model identification, vector fitting, small-signal stability

Abstract

During an offshore wind power plant (OF-WPP) development, various equipment vendors such as STATCOMs and synchronous condensers provide a full-scale black-boxed model of their components to prevent their intellectual property and to avoid unwanted changes in the internal control structure and parameters. Such models are utilized for various time-domain studies; however, insights into small-signal and converter-driven stability miss out due to the lack of small-signal models. In order to perform a small-signal stability study of the entire OF-WPP with the possibility of extracting stability information from the black-box model components, advanced methods such as vector fitting are required. Vector fitting estimates the state-space model of the black-boxed system component from which the overall state-space model of the OF-WPP can be built, thus facilitating an overall small-signal stability analysis, which can provide insights into the source of system instability via modal analysis. This paper presents the application of vector-fitting methods on various OF-WPP components from their immittance scans to estimate the small-signal model of the component. A validation of the vector fit results against EMT-based and frequency domain model (FDM) based immittance scans are provided to demonstrate the accuracy of the proposed method. The results show that crucial model information can be extracted from the immittance scans of the black-boxed component models without the vendors needing to provide IP-protected internal model parameters explicitly. The extracted model information can be utilized for the overall small-signal stability analysis of the WPP.

1 Introduction

In recent years, power systems have transformed from traditional synchronous-machine-based generators to converter-based ones. This shift increases the complexity of modern power systems, which are increasingly defined by intricate control configurations and multiple interacting components that require careful coordination among various stakeholders, including original equipment manufacturers (OEMs) and developers [3]. In recognition of this fact, converter-driven stability has been added as a fundamental category of power system stability [6]. For instance, modern wind power plants (WPPs) can be comprised of dozens of large wind turbines (WTs), active compensation devices such as STATCOMs, and long-distance HVDC transmission systems, necessitating close collaboration among multiple OEMs and developers to manage interactions and maintain stability.

Small-signal stability is of particular interest when investigating the stability of such multiple interconnected systems. There are several ways to assess small-signal stability. For example, impedance-(or admittance-) based analysis is a popular method that evaluates the stability of an interconnected system by using the ratio of the subsystem impedances at the node being studied [3]. However, this method only provides information on a local operating point and may hide the dynamics of the internal subsystems, which may be significant at other operating points [2]. Generally, the impedance-based analysis method also lacks an appropriate method for dealing with multiple operating points [13]. On the other hand, Eigenvalue-based stability analysis is a method in which the state-space model of the system under study is made available, and the eigenvalues of the state-matrix are analysed. The eigenvalue-based method allows for participation factor analysis to discern the origin of system instability and is therefore favoured when investigating the compatibility of interconnected systems [3].

Creating a state-space model representation of a component is a difficult process, which many OEMs do not have the capacity to do, both due to the difficulty involved and the lack of standardization within the industry. Additionally, OEMs need to protect their intellectual property and frequently supply only a black-boxed (BB) electromagnetic transient (EMT) model to transmission system operators (TSOs) and collaborators. This calls for a system-identification technique that can readily produce state-space models from BB EMT models in a fast and relatively simple way. One such technique, the vector fitting (VF) method, has recently gained prominence in the power systems field for this purpose, as vector fitting is relatively simple and computationally efficient. However, the accuracy of the state-space models constructed using the VF method and their utility when analysing small-signal stability are still being assessed. The aim of this paper is, therefore, to build on current knowledge of the method and establish the method's effectiveness. First, the three different versions of the vector fitting method for MIMO systems will be compared. The effect of noise on the resulting model is additionally analysed. Finally, the usefulness of the methods for conducting small signal stability analysis will be assessed.

Section 2 outlines the theory of vector and matrix fitting methodologies existing in the literature and model order determination methods to be used. Section 3 shows the setup for immittance scans in PSCAD, which are taken to get a realistic immittance scan of a BB EMT model of a power generating unit (PGU). In Section 4, to evaluate the matrix fitting methodologies, the admittance scan is vector-fitted and benchmarked against an equivalent FDM of the same PGU. Each VF and matrix fitting (MF) method is evaluated by benchmarking the pole plots of the FDM vs the generated state space models. Section 5 tests the use of the VF-generated state-space models for stability analysis by setting up two WPP systems, including a STATCOM, in order to benchmark the stability of the two VF-generated state-space models.

2 The Vector Fitting Method

Vector fitting is a method for approximating a pole-residue model (1) of a frequency response input using least-squares approximation. The model is assumed to be rational and is defined by N poles, p_n, residues, and c_n, which can be complex or real quantities. d and h are real quantities and can be zero [5].

$$f(s) = \sum_{n=1}^{N} \frac{c_n}{s - p_n} + d + sh \tag{1}$$

The model is approximated using a set amount of complex poles to the frequency response input, relocating them iteratively using the least squares approach and then calculating the residues. The resulting model can then be converted into a state-space form. Among the most important factors to consider when using the vector fitting method are the following:

- **Model order selection:** The model order is most often determined by simply increasing the order until the root-mean-square error (RMSE) of the frequency response fit decreases to an acceptable level. This approach may be augmented by analyzing the frequency response to estimate the correct order. The goal should be to minimize the model order so that non-existent dynamics are not introduced. In this paper, several model order reduction methods are introduced.
- **Passivity and stability enforcement:** Depending on the modelled system, it may be desirable to enforce model stability or passivity. In the case of active devices, passivity should not be enforced. On the other hand, stability is an attribute enforced when the system in question is *known* to be stable. In the case of measurement data, a stable operating point is found to measure the device's immittance frequency response. This requires one to use stability enforcement [11].
- **Measurement noise:** In most cases, the vector fitting method handles noise well. However, results vary when applied to *multiple-input-multiple-output (MIMO)* systems, as discussed in this study.

2.1 Use on MIMO Systems

The standard vector fitting method may be applied to single-input-single-output (SISO) systems. However, different applications of the method exist for MIMO systems, which are discussed in [4]. The variation lies in how poles are shared between input matrix elements. For example, for a $2 \times 2 \times N$ input matrix, one may distribute the model poles in multiple ways. The most common method, Matrix Fitting, shares a single pole set across all inputs. This is the most efficient method and is, in most cases, sufficient. However, it is assumed that the individual inputs share common resonance peaks, with little variation in their behaviour. One may choose to model each column of the input matrix separately or even model each input element individually to capture those differences.

2.1.1 Matrix Fitting: In the case of a $P \times P$ input matrix, instead of a scalar element input, the pole-residue model output by the VF method, introduced in (1), is adjusted accordingly:

$$\boldsymbol{H}(s) = \boldsymbol{R}_0 + \sum_{n=1}^{N} \frac{\boldsymbol{R}_n}{s - p_n} \tag{2}$$

A common pole set is fitted to all responses of the matrix $\boldsymbol{H}(s)$ [4]. It is, however, the residue matrices $\boldsymbol{R_n}$, as well as the standard $\boldsymbol{D}$ and $\boldsymbol{E}$ matrices of a state-space model, which give the differences between the different elements of $\boldsymbol{H}(s)$ [10]. With this method, the number of states in the resulting model is $N = P \cdot n$, meaning the number of poles n multiplied by the number of ports P. This results in an $N \times N$ size $\boldsymbol{A}$ matrix, which is larger than the actual dynamic order of the model.

2.1.2 Muilti-SISO and Multi-SIMO: Most other methods differ in the degree to which poles are shared between inputs. Two methods, the Multi-SISO, Multi-single-input-multiple-output (SIMO) and MF methods, are established in [4] along with MF. The multi-SISO method splits the entire input matrix into individual elements, extracting SISO models for each scalar with poles and residues. For a $P \times P$ size input matrix, the multi-SISO method constructs the models in the following way:

$$H_{ij}(s) = R_{ij,0} + \sum_{l=1}^{N_{i,j}} \frac{R_{ij,l}}{s - p_{ij,l}}, \quad i, j = 1, ..., P \tag{3}$$

Given that each SISO model has the same number of poles n, the total number of poles for a $P \times P$ becomes $N = P^2 n$. A system state-space realization is constructed after converting these individual subsets into state-space models, combined

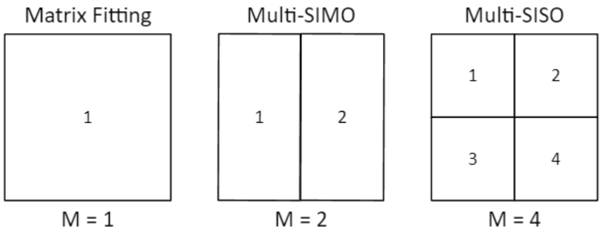

Fig. 1: Illustration of three common pole splitting strategies for a system with $P = 2$ ports. M signifies the number of independent submodels calculated by the method, which are later combined into one model.

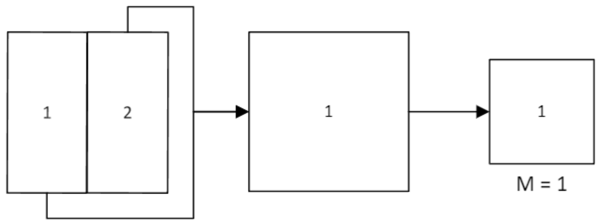

Fig. 2: PC-CF method diagram for a system with $P = 2$ ports. The columns are first fit with a high order. Their pole sets are then combined into one after which the clustering method is used to reduce the model order.

into one, as described in [4]. This method may apply to MIMO systems with a significant disparity between input responses. However, it has the limitation of producing more non-vanishing matrix elements.

The multi-SIMO method, on the other hand, offers a more compact modelling result than multi-SISO while capturing more differences between outputs than MF. Instead of generating a model for each element, this method splits the system into columns. Denoting $h_j(s)$ as the jth column of the transfer function $\boldsymbol{H}(s)$, the multi-SIMO method constructs a model structure:

$$H_j(s) = r_{j,0} + \sum_{l=1}^{N_j} \frac{r_{j,l}}{s - p_{j,l}}, \quad j = 1, ..., P \tag{4}$$

P submodels are thereby constructed, each driven by an individual input. The system model $\boldsymbol{H}(s)$ is therefore:

$$\boldsymbol{H}(s) = h_1(s), h_2(s), ..., h_P(s)$$

This model has $N = P \cdot n$ poles, given a constant number of poles for each column. The differences between the three methods are shown graphically in Figure 1.

2.1.3 PC-CF Method: A Pole collapsing-column fitting (PC-CF) method is proposed in [12]. Combining aspects of the Multi-SIMO column fitting method with the MF method: this method entails calculating a pole set for each column and "collapsing" the pole set into a single set representing the entire system. This method is meant to increase the accuracy of pole placement and simplify model order selection. After calculating the pole sets for each column of the input matrix, the total pole set is given as a union of them all:

$$P_{init} = \cup_{i=1}^{I} \cup_{n=1}^{N} p_{i,n} \tag{5}$$

Using a relatively high number of starting poles for each column, essentially *overfitting* each entry, the method states that the dominant poles will become convergent while the rest will be random or are fitted to noise in the data. In this way, the dominant poles will be common between each column and can be identified by the degree to which they overlap with other poles, with a set tolerance. This identification method is highly customizable, requiring the user to select the initial number of poles fit to the columns and adjust the tolerance with which the poles overlap. The number of initial poles must exceed the expected order of the model, as fitting more poles increases the chance of identifying pole clusters. In [12], the tolerance value is taken as a percentage of the real and imaginary components of each pole, thereby scaling the tolerance based on proximity to the origin. This allows for high relative accuracy regardless of a pole's frequency and damping. The tolerance value usually lies between 1% to 10%, depending on the concentration of resonance poles in the input matrix. This tolerance value was found to be too constraining on poles close to the origin, as the overlap tolerance area becomes exceedingly small. A minimum tolerance level of 1Hz is therefore added to this value, such that low-frequency values are captured more reliably by this method.

For a system with $P = 2$ ports, if at least two poles are within the rectangular area determined as the tolerance boundary, the pole is treated as a cluster and kept for the combined pole set. The pole closest to the median of the same cluster is then taken to be the representative pole, with the others being deleted from the set. Poles not identified as belonging to a cluster are similarly deleted from the pole set, significantly reducing the internal states.

2.2 Model Reduction

Selecting the appropriate model order for the vector fitting method has been discussed since its initial development [5]. Balanced truncation is a method that has shown great promise in this regard and will be expanded on shortly in this section. Compared to other methods, findings have shown it to be among the most effective at reducing model order while maintaining accuracy [9, 12].

Balanced truncation is a common technique for order reduction of state-space systems. By using the Hankel Singular Values (HSV) of the system, the "highest energy" poles can be retained, thus reducing pole repetitions and better retaining the behaviour of the system [12]. Figure 3 shows a flowchart for the model compaction process using balanced truncation. HSVs, $\boldsymbol{\sigma}_H$, are the square root of the eigenvalues of the product of the state-space model's controllability grammian $\boldsymbol{W}_C$ and the observability grammian $\boldsymbol{W}_O$ from (6). These two matrices can be found as the solutions to the Lyapunov equations, detailed in [12, 9].

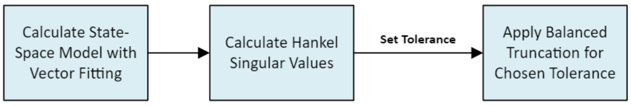

Fig. 3: Model reduction using balanced truncation.

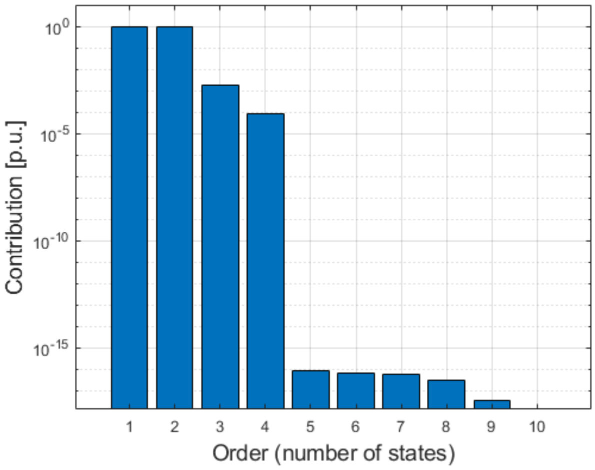

Fig. 4: Hankel singular values of an overfit example system. The first four states contribute the most to the system dynamics. Note that the y-axis is logorithmically scaled.

$$\sigma_H = \sqrt{eig(\boldsymbol{W}_C \boldsymbol{W}_O)} \tag{6}$$

The HSVs' magnitude indicates each state's relative importance to the system's input-output dynamics and, thereby, a suitable order for the system in question. Balanced truncation identifies which HSVs fall below a threshold ρ defined by the user and deletes the corresponding states from the system. This process simplifies the system so only the "strongest" poles remain. The value of ρ is set to be equal to the value of the HSV associated with the desired rank r [9].

$$\rho = \sigma_{H,r} \tag{7}$$

This requires one to calculate the HSVs of the system, identify the mode number at which the HSV values drop, and adjust ρ accordingly. In most cases, the drop in HSV magnitude is readily apparent, as is seen in Figure 4. However, when working with a larger system, the drop in magnitude may be more gradual, in which case one must either lower the model order of the fit or rely on engineering judgment when choosing the desired model rank.

3 Admittance Scans Setup & Results

The admittance data is calculated in the dq-domain in PSCAD by injecting current perturbations into the converter reactor and measuring the voltage on the grid side of the grid filter, as shown on Figure 5. The immittance data is extracted from the FDM. The perturbation magnitude of the Immittance Scanner is varied to find the minimum magnitude that reduces

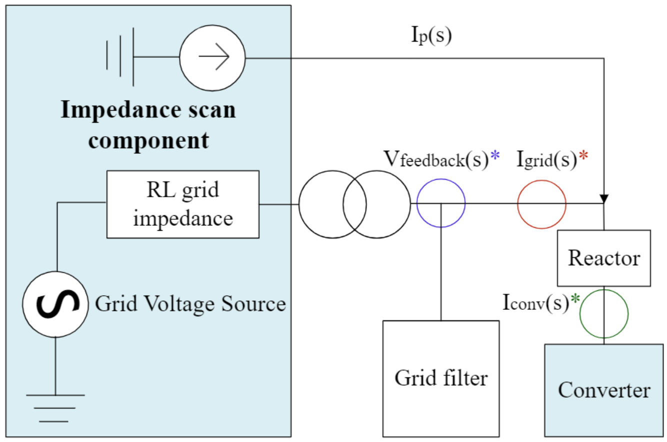

Fig. 5: EMT Immittance Scanner setup *indicates measurements

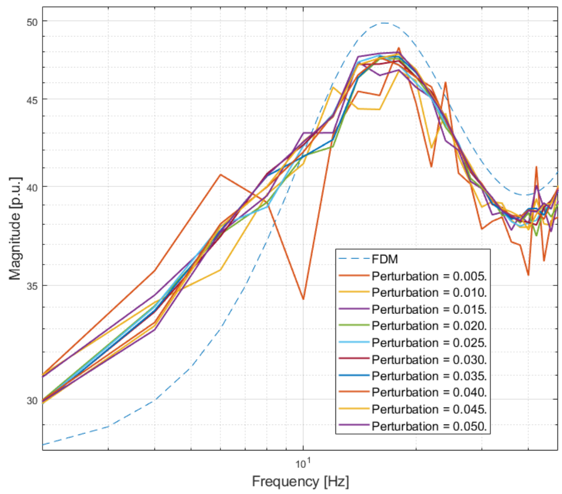

Fig. 6: FDM admittance vs EMT model admittance with different current perturbation magnitudes

noise/discontinuity of the resultant Immitance data; these measurements are seen in Figure 6, where the admittance data of the FDM and of the EMT data at different perturbation magnitudes are benchmarked. The EMT simulation immittance data is noisier/more discontinuous than the FDM data.

Running immittance scans in PSCAD is generally highly computationally intensive, as total simulation time increases significantly as the frequency step size decreases, as both the measurement time at each frequency increases and the number of increments also increases. The parameters of the immittance scan EMT simulations are outlined in Table 1; these are chosen to strike a balance between computation time and retaining as many important system poles as possible, as well as focusing on the lower frequencies below $f_s/2$, as control loop interactions and harmonic resonance oscillations are of greater interest than switching harmonics.

The resultant admittance shown in Figure 7 shows that the EMT measurement data is more noisy/discontinuous than the

Table 1 Immittance scan parameters

Parameter	Value
Perturbation magnitude I_p [p.u.]	0.025
Frequency range F_{range} [Hz]	1-1200
Frequency step size F_{step} [Hz]	1
Duration of measurement at each step T_{delay} [s]	2

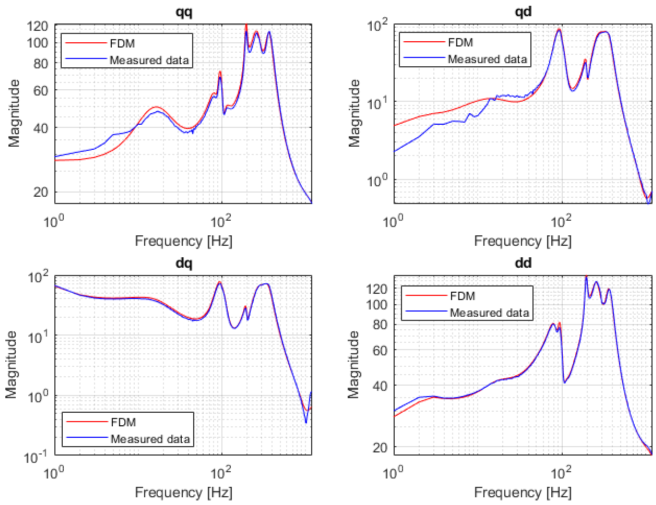

Fig. 7: FDM admittance vs EMT model admittance in the dq domain

FDM data. Figure 7 indicates which MIMO vector fitting method may work best in this input data. MIMO frequency response data sharing common resonances is best fitted using the matrix fitting method or the PC-CF method, as those methods fit a single pole set to the whole system. This is opposed to methods such as the multi-SIMO method, which fits each input matrix column individually, and the multi-SISO method, which fits each input element individually. Those two methods are best suited for systems with a high degree of variation in their frequency inputs. Observing Figure 7, there is some commonality in the resonance peak frequencies across inputs. Therefore, the MF and PC-CF methods are likely to be most applicable to the input data. However, as there is also some variation, especially in the measurement data, comparing those methods against the multi-SIMO method might also yield good results.

4 FDM Benchmark Evaluation

Three MIMO vector fitting methods are tested and compared using the PSCAD-based model of the WTG converter discussed previously. Additionally, a white box FDM model of the same device is used to compare with the EMT model for further comparison. While the frequency response data is not exactly the same, as is shown in Figure 7, this comparison is included to show the vector fitting method's performance using data with different degrees of fidelity. First, the three methods are used on both sets of frequency response data for a total of six models. The trial and error method is used initially, after

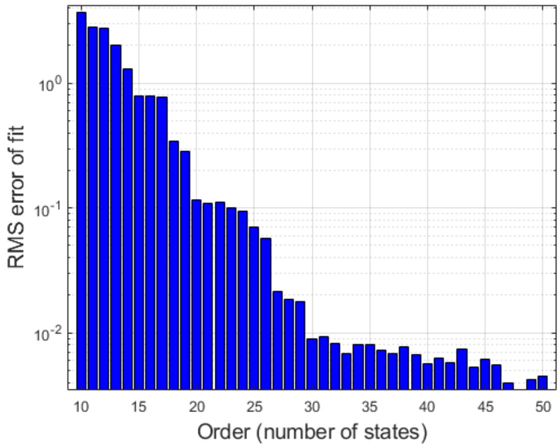

Fig. 8: RMSE of model fit against frequency response input vs number of states (model order). After the order reaches 30 the RMSE decrease is marginal.

which the models are reduced using balanced truncation. The six models are then compared using two measures: the error of the vector fit model fit compared against the input data and by direct comparison with the white box FDM eigenvalues. The later comparison involves first connecting the vector fit model to an impedance model, which may be directly compared to the white box model. This type of comparison is not available in the case of true black box models, though it is done in this case to test the accuracy of the vector fitting methods.

4.1 Initial Model Construction

The trial and error method is used for the three MIMO vector fitting methods: Matrix fitting, multi-SIMO and PC-CF. The trial-and-error method is used to decide the initial order. For the Matrix Fitting and multi-SIMO methods, the model order is simply increased until improvements in fit error are marginal or plateau. The RMSE of the fit magnitude is used as a measure of accuracy and is calculated in the following way.

$$\text{Fit RMSE} = \sqrt{\frac{1}{N}\sum_{s=1}^{N}|f(s) - g(s)|^2} \tag{8}$$

However, a different approach is taken for the PC-CF method, as the model order decided on is already an overfit of the model. Therefore, the overlap tolerance percentage is increased from 1% to 10%, effectively increasing the size of the resulting model. An example of this process for the matrix fitting method is shown in Figure 8. Figure 9 shows the same process for the PC-CF method.

The resulting model orders of the matrix fitting and multi-SIMO models are shown in Table 3. The PC-CF model order is set by the tolerance percentage chosen for each frequency response input, which is set to be 3% for the FDM data model and 10% for the measurement data model. Note that the PC-CF model of the measurement data has to include a much higher tolerance order to model the more noisy measurement

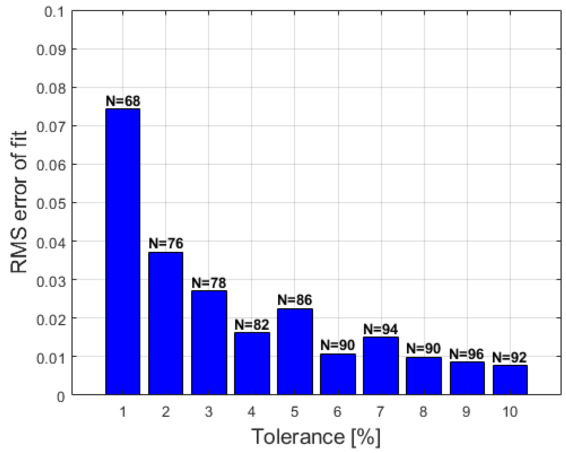

Fig. 9: RMSE of model fit to frequency response input against tolerance percentage. The error decreases as the tolerance percentage increases, though the model order increases in turn.

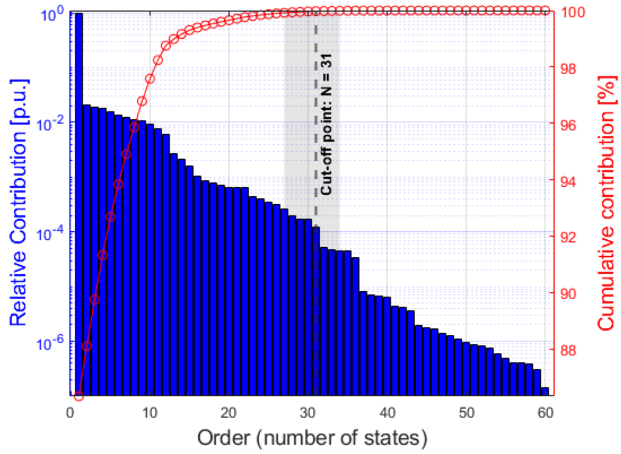

Fig. 10: Magnitude of the Matrix Fit model of the FDM produced frequency response HSVs vs the model order. Note that the y-axis is scaled logarithmically.

Table 2 RMSE comparison between the three multiport vector fitting methods.

Fitting Method	**Fit RMSE**	
	FDM data	Measurement data
Matrix Fitting	0.0089	0.4544
multi-SIMO	0.0070	0.4483
PC-CF	0.0270	1.5806

data input more accurately, highlighting a potential weakness of that method. The fit error of the initial model order is shown in Table 2. Notably, the matrix fitting and multi-SIMO methods perform at a similar error rate, with the multi-SIMO method achieving a slightly lower RMSE than the Matrix Fitting method. The PC-CF method, on the other hand, has a far greater RMSE than the other two methods. Additionally, as is to be expected, the models of the FDM data have a better fit than those of the measurement data due to the FDM data's lack of measurement noise.

4.2 Model Reduction and Accuracy Assessment

The resulting models are then reduced using balanced truncation. The degree to which the models are reduced depends on the percentage of model dynamics covered by the existing states and one's engineering judgment. Figure 10 shows an example of this approach. Through experience and observation, it is determined that the result should maintain at least 99.90% of the original model dynamics, which, as seen in the figure, allows one to reduce the model by around half.

The results of the model reduction can be seen in Table 3.

Table 3 Initial model order and model reduction results for all three VF methods.

Method	**Data type**	**Orig. order** (N states)	**Red. order** (N states)	**Percentage Red.**
MF	FDM	60	31	48%
	Meas.	60	31	48%
multi-SIMO	FDM	60	36	40%
	Meas.	60	41	32%
PC-CF	FDM	78	34	56%
	Meas.	56	50	11%

If this were a black box model, initial model development would stop here. However, as the white box model of the system is available, the accuracy of the three methods for the FDM data and measured data can be assessed. As the focus of this study is on the low-frequency, low-damping end of the frequency range, the accuracy of the model in that particular area will be assessed using a novel method based on one [12, 10].

First, a "target area" is defined to assess the model's accuracy. This is done to focus the accuracy assessment on a specific frequency and damping range. Next, the VF model eigenvalues, which overlap with the white-box eigenvalues within a pre-set tolerance, are identified. The tolerance value is set to be a percentage of the white-box model eigenvalues, with a minimum tolerance value of 2 Hz for the imaginary axis and 2 sec^{-1} for the real axis. This is similar to the cluster identification method used for the PC-CF method. Next, the mean Euclidian distance between the identified white-box poles and the corresponding white-box poles is calculated using Equations (9) and (10). In these equations, p_i contains the identified white-box model poles, c_i contains the corresponding VF model poles, and N is the number of identified poles.

$$d_i = \sqrt{(\mathrm{Re}(p_i) - \mathrm{Re}(c_i))^2 + (\mathrm{Im}(p_i) - \mathrm{Im}(c_i))^2} \quad (9)$$

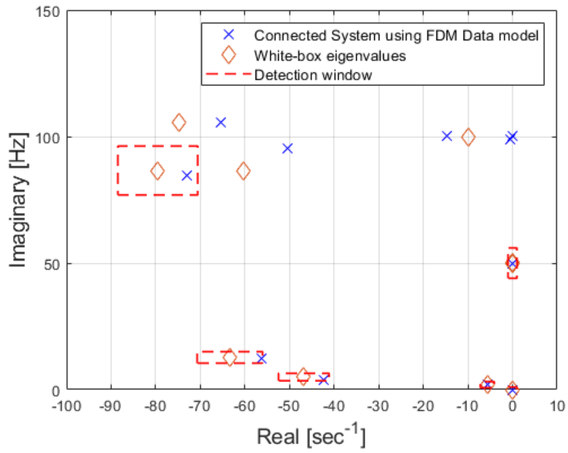

Fig. 11: Accuracy evaluation example, using the MF model of the FDM produced data. A tolerance zone is defined for each white-box eigenvalue, with a minimum zone size of 1 (Hz or sec^{-1}). Should a VF model eigenvalue fall within that zone, the zone is plotted, and the corresponding white-box eigenvalue is listed as "identified". Since the detection window size is a percentage of the eigenvalues' real and imaginary components, its dimensions may vary drastically based on the value location.

$$\text{MEAN}(d_i) = \frac{1}{N}\sum_{i=1}^{N} d_i \tag{10}$$

The mean of the Euclidean distance, along with a tally of how many poles are identified, is presented as a measure of model accuracy. While being slightly more convoluted than others, this accuracy assessment method results in a highly targeted measure that informs both how many poles are correctly identified and the mean of the Euclidean distance of those identified poles within a specific frequency range. This can be useful when, for example, investigating sub-synchronous modes in the system, as only those eigenvalues within the area of interest are considered. Figure 11 shows an example of this accuracy evaluation method.

The focus of this assessment being on the lower frequencies, the target area is set to $150Hz$ and 100 sec^{-1}, which should capture the outer control loops. This aligns with assessments of a similar nature and focuses on those poles with low frequencies and low damping [2], which are of particular concern when assessing the stability of this nature. For all models, a tolerance value of 10% is set. Table 4 shows the accuracy assessment results.

Table 4 Model verification results for EMT and FDM data. Two measures are included: the mean of the Euclidean distance of the identified poles and the number of poles identified.

Fitting Method	**Mean Distance**		**Poles Identified**	
	FDM	Meas.	FDM	Meas.
Matrix Fitting	3.142	4.358	10/13	8/13
Multi-SIMO	2.489	2.230	9/13	9/13
PC-CF	1.750	3.352	10/13	6/13

For all methods, those models produced by the FDM Data result in the closest fit to the white-box model of the PGU converter. This was expected, as the FDM Data represents the ideal data input. More surprising, however, is the fact that, of the three methods, the PC-CF method results in the most accurate fit, despite having had one of the worst average distances when fit against the input frequency response, as is seen in Table 2. This indicates that, even if a method provides a worse frequency response fit, it may match the system dynamics as well as comparative methods, depending on the area of focus. In this case, that area is the lower frequency range, which the PC-CF matches quite well, both in terms of average distance and number of poles identified. For the other two methods, the multi-SIMO method performs better while identifying one less pole than the MF method. The MF method identifies as many poles as the PC-CF method, with a higher average distance.

Another notable result is the poor performance of the PC-CF method in modelling the measurement data, where it only identifies 6/13 poles in the target area. This is likely due to the methods' relative susceptibility to measurement noise.

The accuracy assessment results bring to light the advantages and disadvantages of each MIMO vector fitting method. The Matrix Fitting method appears to perform well on average. It identifies as many poles as the PC-CF method using the FDM data and almost as many as the multi-SIMO method using the Measurement Data. It does, however, have a high average distance compared to the other methods. The multi-sIMO method performs similarly to the Matrix Fitting method, identifying 9 out of 13 poles for each model. Additionally, it has a low average distance for both models and notably has a lower distance value when using the measurement data. Finally, while scoring the highest accuracy when using the FDM-produced data, the PC-CF method fails to replicate similar results when using the less optimal measurement data. Therefore, one may conclude that the multi-SIMO method performed the best on average and exceptionally well for the Measurement Data. This results from the method's ability to fit the columns of the input matrix individually, allowing for more accurate pole placement in case of noisy data. However, the other two methods returned more favourable results for the FDM data input, with the PC-CF showing the most significant promise.

When comparing these results with the frequency response fit RMSE for each method, seen in Table 2, they appear to correlate for the MF and multi-SIMO methods. The multi-SIMO method outperforms the MF method, though they are comparable in accuracy. The PC-CF method, however, does not

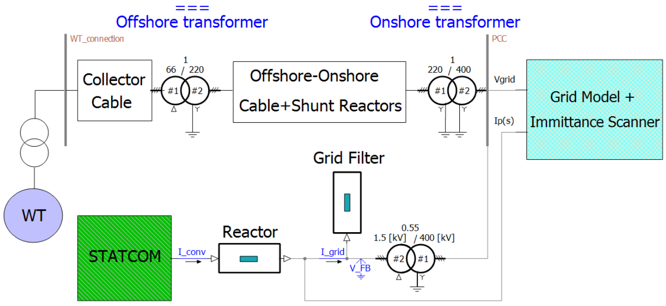

Fig. 12: Setup of WPP

Table 5 WPP setup and STATCOM operating point values in per unit

Parameter	System 1 [pu]	System 2 [pu]
Grid SCR PCC	10	10
XR ratio PCC	14	14
SCR WT transformer	2.5	1.5
XR ratio WT transformer	14	6.56
$V_{AC,ref}$ STATCOM	1.054	1.054
$V_{DC,ref}$ STATCOM	3.675	3.16
Q_{meas}	0.86	1
Mod. index STATCOM	0.83	1

correlate well with its fit RMSE when looking at the FDM Data model. The eigenvalue identification accuracy of the method is the greatest of the three methods, though according to the fit RMSE, it fares the worst. A possible explanation for this is that this chapter's measure of accuracy focuses on the lower frequencies, while the fit RMSE considers the whole spectrum. The consequence of this non-correlation when using the PC-CF method is that it is difficult to evaluate whether it accurately identifies the system poles of interest when modelling a black-box system. However, the results for the multi-SIMO and Matrix Fitting methods appear to align with the response RMSE.

5 Black Box Model Setup

In order to showcase the VF methodology's ability to effectively identify a state space model which can be used for eigenvalue-based stability assessments in the small-signal domain, the method is used on the EMT simulation model of a STATCOM connected to the point of common coupling (PCC) of a wind power plant (WPP). An impedance scan of the interconnected system is done at the STATCOM terminal. The resultant impedance scans of the grid+WPP and STATCOM will be used to generate two state space models, which will then be connected, and the stability of the interconnected system will be evaluated.

Two system setups are utilized here: system 1, where the STATCOM is operating at below-rated power and the short circuit ratio (SCR) of the WPP is 2.5, and system 2, where the STATCOM AC voltage control will be saturated and the SCR of the WPP will be 1.5. Changing the WPP SCR will be achieved by increasing the offshore-onshore cable length. The AC voltage control is saturated by lowering the DC voltage reference until the STATCOM exports rated reactive power at a modulation index of one. Both these setups are represented by the topology in Figure 12, and the main system parameters are outlined in Table 5.

5.1 Stability Analysis

Both systems' immittance scans are measured in EMT simulations; therefore, both systems are assumed to be stable, as meaningful scan results would not be possible if the systems were unstable at the given operating points [10, 2]. The objective of this analysis is stability evaluation; however, with the stability enforcement limiting the eigenvalues with positive real parts, this paper instead evaluates underdamped eigenvalues with a damping ratio below a specified level. Generally, the damping ratio of electromechanical oscillation modes needs to be greater than 0.05 before the power system operation is acceptable [8, p. 536], in [1] a marginally stable converter based system is analyzed with a minimum damping ratio of 0.008. A novel threshold for our context is 0.02; modes with a lower damping ratio will be considered critical modes. It should be noted that this threshold is a heuristically selected value based on our context.

The appropriate MIMO vector fitting variants are selected based on an analysis of the the immitance frequency responses of the Grid+WPP and the STATCOM for both systems. The multi-SIMO method is used on the STATCOM of System 1 due to variations in its response inputs, while the Matrix Fitting method is used on the System' Grid+WPP. The matrix fitting method is used on both subsystems of System 2.

The Grid+WPP and STATCOM VF state space models for both systems are connected using the `connect` function in Matlab, which outputs a single system SS model, where the state names from the individual systems remain such that a participation factor analysis can be done on the origins of critical modes. The pole plots for the VF systems are collected in Figure 13.

The VF state space models are derived from a fit transfer function; thereby, one can make an arbitrary selection of the state variables of the state-space model [7, p. 719]. However, the subsystem origin of each state can be determined. Thus, subsystem contributions to critical modes can be found by summing the subsystem states normalized participation factors to critical modes. Table 6 outlines the number of critical modes in Figure 13 and each subsystem's contributions to the identified critical modes.

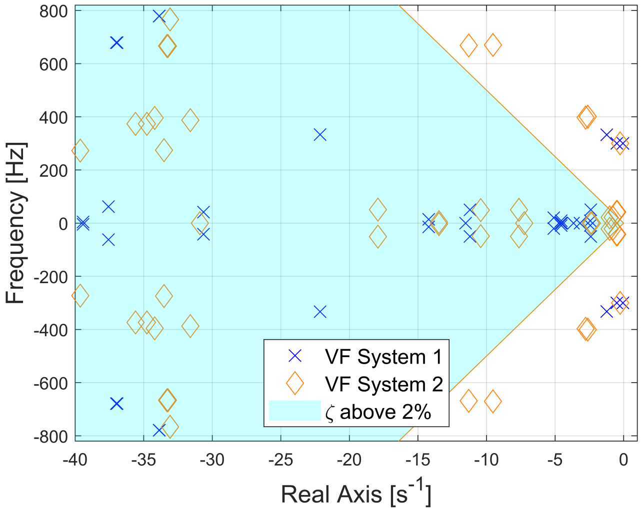

Fig. 13: Pole plots for VF systems state-space models with grid topology from Figure 12 and operating points as in Table 5, the cyan area is for modes with a damping ratio above 0.02.

Table 6 Critical mode origin of VF System 1 and VF System 2

	VF System 1	**VF System 2**
Critical mode pairs	3	7
STATCOM contribution	24.6%	47.9%
Grid+WPP contribution	75.4%	52.1 %

Table 7 and 8 show values of the identified critical modes for the VF System 1 and 2, respectively. It appears that saturating the AC voltage control of the STATCOM introduces two pairs of critical subsynchronous pole pairs, and having a lower SCR in the WPP reduces the damping of some higher-frequency pole pairs. The specific dynamics behind the lower damping of these poles are not investigated in this paper.

Table 7 Critical modes of System 1

Modes	ζ	**Freq.**	**STATCOM**	**Grid+WPP**
20 & 26	0.00370	332	0.2	0.8
24 & 30	0.00166	300	0.21	0.79
23 & 29	0.000175	299	0.33	0.67

Table 8 Critical modes of System 2

Modes	ζ	**Freq.**	**STATCOM**	**Grid+WPP**
14 & 7	0.014200	670	0.1	0.9
15 & 8	0.016900	668	0.33	0.67
20 & 29	0.006532	400	0.38	0.62
30 & 21	0.006980	398	0.35	0.65
34 & 25	0.000870	300	0.4	0.6
50 & 48	0.011300	42	0.91	0.09
51 & 49	0.012300	41.69	0.93	0.07

6 Conclusion

In this paper, we have outlined the different vector fitting methodologies and evaluated each of these methods by benchmarking the generated state-space models with a white box commercial FDM model from SGRE. The VF methodologies have shown promising results in identifying the low-frequency and low-damping poles of the model. However, it is crucial to select the VF methods with caution, considering the commonality across DQ immittance scans and the quality of the measurement data. For instance, the PC-CF method is more sensitive to noisy/discontinuous data than the other methodologies. This emphasis on careful selection is important to ensure the accuracy and reliability of the VF methodologies in power system stability and control.

The frequency data is gathered by performing immittance scans of EMT simulation models via an internal SGRE PSCAD Impedance Scanner component. A WPP model with a STATCOM is analysed in two system setups, with one system operating closer to stability limits than the other. The stability of the VF state space models is found to reflect the expected relative stability. Additionally, participation factor analysis is used to quantify the contribution of each component to the observed instability. These studies are very preliminary, and further analysis needs to be made to confidently assess this stability evaluation's legitimacy.

7 Legal Disclaimer

Figures and values presented in this paper should not be used to judge the performance of Siemens Gamesa Renewable Energy technology as they are solely presented for demonstration purposes. Any opinions or analyses contained in this paper are the opinions of the authors and are not necessarily the same as those of Siemens Gamesa Renewable Energy.

8 References

[1] Mohammad Kazem Bakhshizadeh et al. "Improving the Impedance-Based Stability Criterion by Using the Vector Fitting Method". In: *IEEE Transactions on Energy Conversion* 33.4 (2018), pp. 1739–1747. DOI: 10.1109/TEC.2018.2849347.

[2] Mohammad Kazem Bakhshizadeh et al. "The Application of Vector Fitting to Eigenvalue-Based Harmonic Stability Analysis". In: *IEEE Journal of Emerging and Selected Topics in Power Electronics* 5.4 (2017), pp. 1487–1498. DOI: 10.1109/JESTPE.2017.2727503.

[3] CIGRE. *Multi-frequency stability of converter-based modern power systems*. Technical Brochure 928. Accessed: 2024-06-20. Paris, France: International Council on Large Electric Systems (CIGRE), 2024. URL: https://www.e-cigre.org/publications/detail/928-multi-frequency-stability-of-converter-based-modern-power-systems.html.

[4] Stefano Grivet-Talocia and Bjørn Gustavsen. *PASSIVE MACROMODELING, Theory and Applications*. 1st ed. John Wiley and Sons, 2016.

[5] B. Gustavsen and A. Semlyen. "Rational approximation of frequency domain responses by vector fitting". In: *IEEE Transactions on Power Delivery* 14.3 (1999), pp. 1052–1061. DOI: 10.1109/61.772353.

[6]Nikos Hatziargyriou et al. "Definition and Classification of Power System Stability – Revisited & Extended". In: *IEEE Transactions on Power Systems* 36.4 (2021), pp. 3271–3281. DOI: 10.1109/TPWRS.2020.3041774.

[7]Prabha Shankar Kundur and Om Prakash Malik. *Power System Stability and Control*. 2nd ed. McGraw-Hill Education, 2022.

[8]Yonghua Song Malcolm Irving Xi-Fan Wang. *Modern Power Systems Analysis*. Springer Science, 2008.

[9]Abner Ramirez. "Vector Fitting-Based Calculation of Frequency-Dependent Network Equivalents by Frequency Partitioning and Model-Order Reduction". In: *IEEE Transactions on Power Delivery* 24.1 (2009), pp. 410–415. DOI: 10.1109/TPWRD.2008.921139.

[10]Atle Rygg and Marta Molinas. "Apparent Impedance Analysis: A Small-Signal Method for Stability Analysis of Power Electronic-Based Systems". In: *IEEE Journal of Emerging and Selected Topics in Power Electronics* 5.4 (2017), pp. 1474–1486. DOI: 10.1109/JESTPE.2017.2729596.

[11]Atle Rygg et al. "Apparent impedance analysis: A new method for power system stability analysis". In: *2016 IEEE 17th Workshop on Control and Modeling for Power Electronics (COMPEL)*. 2016, pp. 1–7. DOI: 10.1109/COMPEL.2016.7556667.

[12]Andrew Macmillan Smith et al. "Improved Pole Placement and Compaction of MIMO Vector Fitting Applied to System Identification". In: *IEEE Transactions on Power Delivery* 39.2 (2024), pp. 1259–1270. DOI: 10.1109/TPWRD.2024.3364836.

[13]Heng Wu, Fangzhou Zhao, and Xiongfei Wang. "A Survey on Impedance-Based Dynamics Analysis Method for Inverter-Based Resources". In: *IEEE Power Electronics Magazine* 10.3 (2023), pp. 43–51. DOI: 10.1109/MPEL.2023.3303104.